Journal of Engineering Physics and Thermophysics, Vol. 81, No. 1, 2008

MEASUREMENT OF CONCENTRATION PULSATIONS IN A SHEAR TURBULENT FLOW BY THE METHOD OF AVERAGED TALBOT IMAGES

M. V. Doroshko, O. G. Penyaz'kov, P. P. Khramtsov, and I. A. Shikh

UDC 532.517.4

The method of two-exposure Talbot photography has been adapted to analysis of the flow structure in a two-dimensional turbulent submerged jet of helium flowing out into an air space and in a gas flow behind the incident shock wave in a shock tube. Measurement of the local shift of the intensity maxima in the time-averaged Talbot image made it possible to determine, for the cases investigated, the two-dimensional array of angles of refraction of light with an error to 5%. The distribution of the averaged refractive index of the medium and the concentration of the gas over the flow field has been calculated by integration of the distributions obtained.

Introduction. The Talbot effect [1] is successfully used for investigation of the hydrodynamic features of flows with phase inhomogeneities [2–13], including turbulent ones [8, 13, 14]. As has been noted in [5, 13, 14], the procedure based on this effect ensures measurement of a two-dimensional array of local angles of refraction of light with a high spatial resolution over the flow field (step to 200 μm) and a sensitivity of up to 10^{-5} rad which is comparable to the operation of high-quality shadow devices. If the exposure time is much longer than the characteristic period of turbulent pulsations in the flow in photographic recording of structural distortions of a Talbot image (talbogram) in the reproduction plane, the instantaneous shift of interference maxima or talbogram elements from the mean position leads to their smearing. Adequate use of the procedure and interpretation of measurement results in this case require that, in instantaneous exposure, the values of the transverse gradient of refractive index in the flow and the intensity and scale of turbulent pulsations in the beam do not disturb the intensity distribution in individual elements of the Talbot image. Then the shift of each interference maximum from its initial position on the undisturbed talbogram can uniquely be related to the average value of the projections $\langle \varepsilon_x \rangle$ and $\langle \varepsilon_y \rangle$ of the local angle of refraction of light onto the coordinate axes. The intensity distribution in the maxima of the Talbot image disturbed by the flow $I(x, y)$ in the case of lengthy exposure will be dependent on the spectral density of pulsations of the refractive-index gradient.

In studying the structure of turbulent and nonstationary flows, the above advantages of the method of two-exposure Talbot photography become even more obvious, when the process of numerical processing of local structural distortions of the Talbot image is ensured. In this case one can obtain fast and accurate information on the average and pulsation values of the refractive-index gradient over the entire flow field. Certain applied capabilities of such a technique in measurements of the averaged characteristics of shear turbulence have been demonstrated in the present work. A two-dimensional vertical submerged helium jet flowing out into an air space and a turbulent air flow in a shock tube, which is formed in interaction of the incident shock wave with turbulizing barriers, were selected as the objects of study.

Experimental Setup. The optical scheme of the setup for measurement of the averaged and statistical characteristics of turbulent flows with a Talbot interferometer has been described in [12–14] in detail. The two-dimensional jet was formed by helium flowing out of a nozzle installed at distance L immediately behind the Talbot grid. The dimensions of the nozzle's outlet cross section were 1.8×40 mm. The helium velocity on the nozzle exist section was ≈10 m/sec. The Reynolds number calculated from the distance from the nozzle exit section was $\mathrm{Re}_l = 4.8 \cdot 10^3$. The

A. V. Luikov Heat and Mass Transfer Institute, National Academy of Sciences of Belarus, 15 P. Brovka Str., Minsk, 220072, Belarus. Translated from Inzhenerno-Fizicheskii Zhurnal, Vol. 81, No. 1, pp. 49–54, January–February, 2008. Original article submitted September 27, 2007.

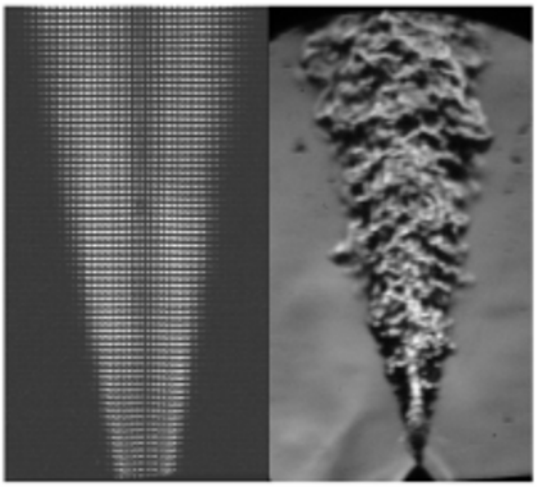

Fig. 1. Difference pattern of the initial and disturbed Talbot image of a two-dimensional jet in the reproduction plane and its shadow photograph.

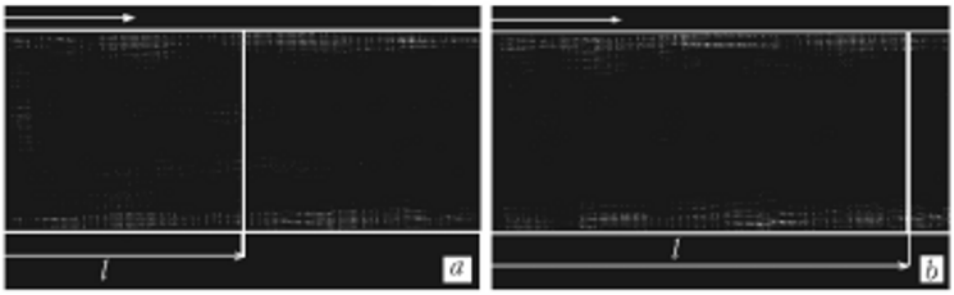

Fig. 2. Difference pattern of the initial and disturbed Talbot image before and after the transmission of light by a turbulent flow behind the incident shock wave (the arrow shows the direction of flow): a) M = 1.32, V = 160.5 m/sec, and l = 124 mm and b) 1.26, 134 m/sec, and 160 mm.

difference (subtractive) flow pattern obtained upon the subtraction of the resulting Talbot image of the jet from the initial intensity distribution in the reproduction plane and the corresponding shadow flow pattern are presented in Fig. 1.

A square shock tube of cross section 50 × 50 mm was used for generation of a shock wave. The interaction of the incident shock wave with turbulizing barriers of different penetrability caused pulsations of the air-flow density and velocity in the test section installed downstream. Grids with square-shaped cells with sides of 3.5 and 12 mm were used to initiate turbulence. The intensity of the shock wave varied within Mach numbers M = 1.26–1.6, which corresponded to an average flow velocity of 134–280 m/sec behind its front. A free-running ruby laser was used for illumination of the Talbot grid. The pulse duration determining the time of exposure of the Talbot image was ≈400 μm. The laser pulse with the instant of arrival of the incident wave at the cross section of recording of the talbogram was synchronized relative to the instant of arrival of the shock wave at pressure transducers installed upstream of a turbulizing barrier.

Figure 2 gives difference images obtained by subtraction of the intensity distribution in the reproduction plane before and after the transmission of light by the turbulent flow behind the transmitted shock wave for grids with dimensions of the cell 12 × 12 mm (Fig. 2a) and 3.5 × 3.5 mm (Fig. 2b). The average velocity of air behind the shock wave was 160.5 and 135 m/sec in these experiments.

It is seen that, along with the local displacement of the talbogram elements over the flow field, which is caused by the average gradient of refractive index in the flow, the interference maxima are substantially smeared because of the presence of turbulent pulsations. The displacement and smearing of the interference pattern are the highest near the tube wall in the dynamic boundary layer developed behind the shock wave.

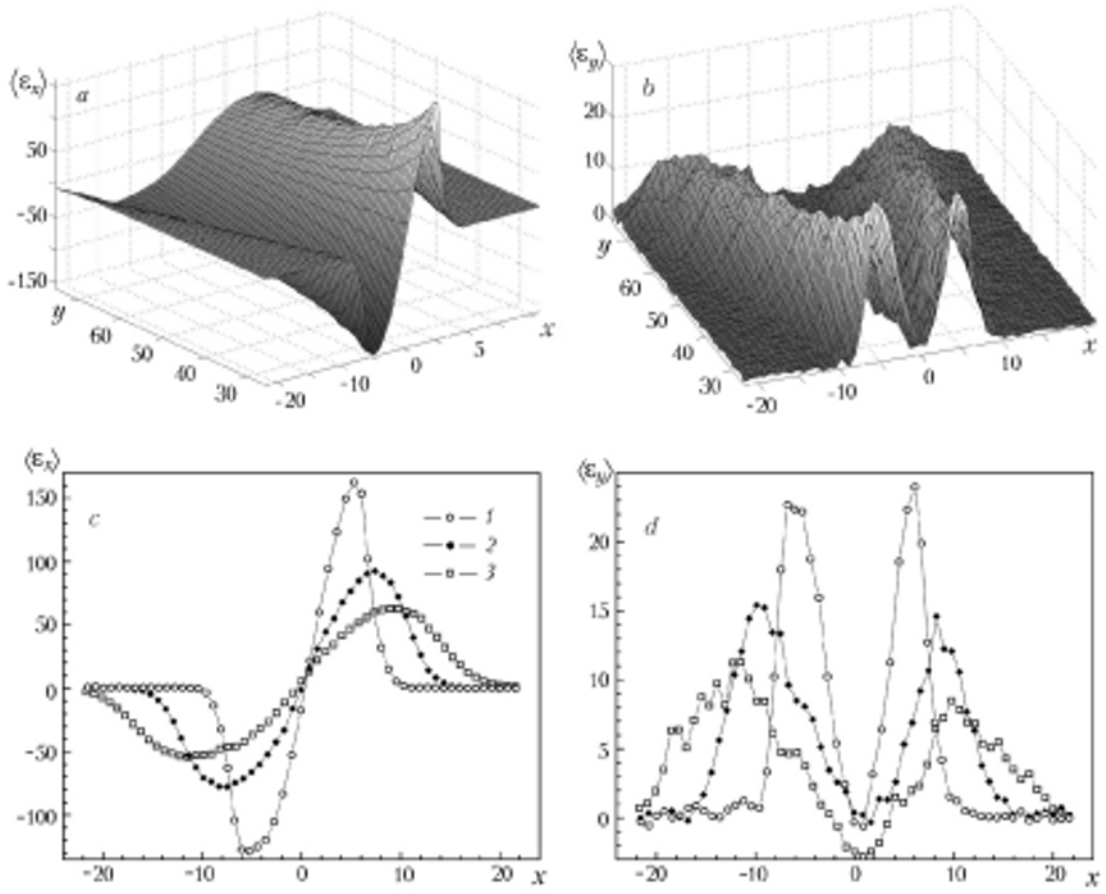

Fig. 3. Distribution of the averaged angles of deflection of light $\langle \varepsilon_x \rangle$ (a and c) and $\langle \varepsilon_y \rangle$ (b and d) in the flow field of the jet: 1) y = 30, 2) 50, and 3) 70 mm. x, y, mm; $\langle \varepsilon_x \rangle$ and $\langle \varepsilon_y \rangle$, seconds of arc.

Determination of the Averaged Concentration of Helium in the Turbulent Jet and Density of Air in the Flow behind the Shock Wave. The distribution of the averaged angles of deflection of light was calculated based on geometrical-optics equations. The computational procedure has been given in [12, 13]. Figure 3 gives results of numerical processing of the two-exposure Talbot photograph of flow for a submerged turbulent helium jet; the calculations have been carried out to determine the local values of the projections of the angle of refraction $\langle \varepsilon_x \rangle$ and $\langle \varepsilon_y \rangle$ onto the coordinate axes. The characteristic extrema corresponding to the boundary layers of mixing of the jet core with the ambient air are clearly seen in the distributions established. The flow core is expanded with distance from the nozzle exit section, and the distributions of the projections of the average angle of deflection become smoother. The pulsations of the longitudinal angle $\langle \varepsilon_y \rangle$ in the mixing layer are more pronounced downstream of the nozzle exit section.

Figure 4 shows analogous dependences measured in transmission of light by the turbulent flow behind a shock wave in the shock-tube's cross sections indicated in Fig. 2. The largest density gradients in the flow behind the shock wave and consequently the largest angles of refraction are observed near the tube walls in the boundary layer. The most appreciable changes in the density and the angles of deflection are recorded in the transverse direction. For the grid with a large cell (12 × 12 mm) (Fig. 4a), the dependence of the projection of the local angle of refraction of light $\langle \varepsilon_x \rangle$ at the center of the shock tube has the form of characteristic pulsations with a period close to a cell step of ≈12–14 mm. Such a dependence for the grid with a small cell (3.5 × 3.5 mm) (Fig. 4b) is flat, in practice.

Two-dimensional distributions of the angles of refraction, which have been established by numerical processing of two-exposure Talbot photographs, can be used to restore the concentration of the gas and the density of the medium. When the value of the refractive index in the undisturbed zone [12, 13] is known, with allowance for the

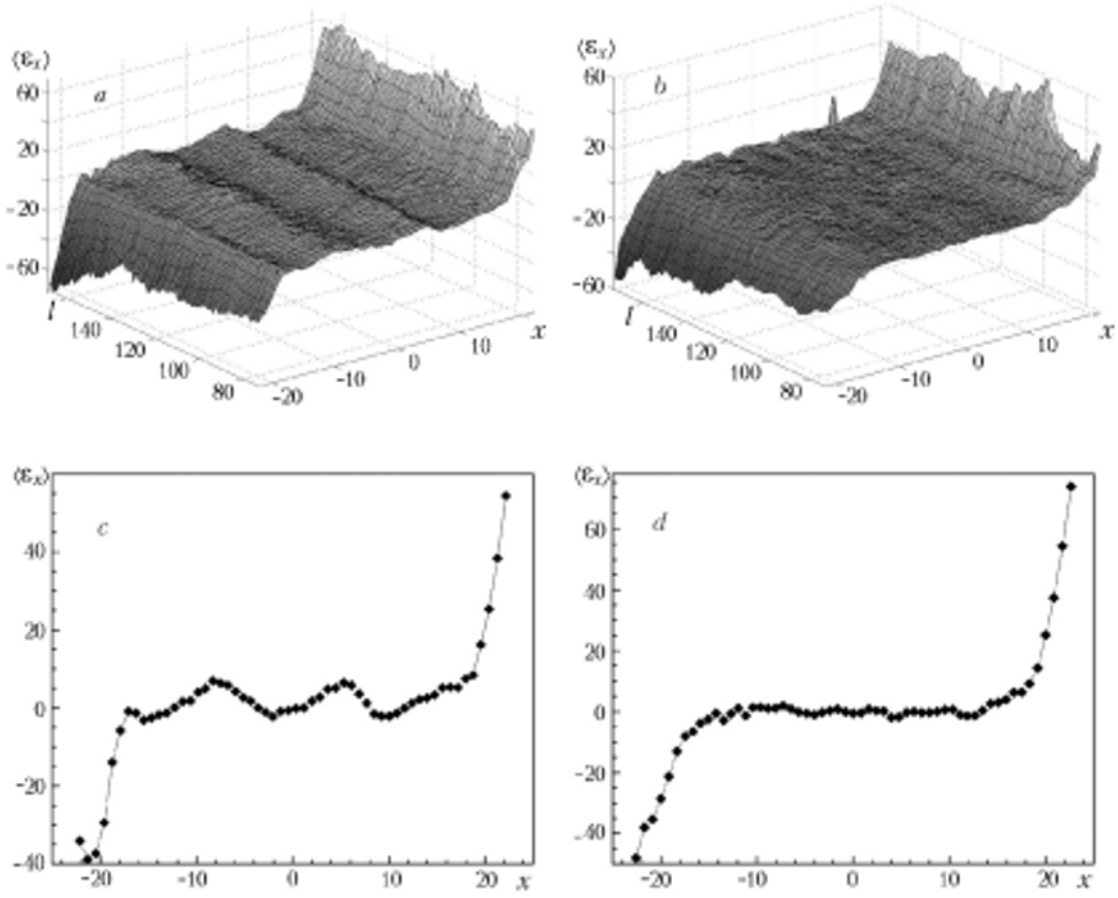

Fig. 4. Distributions of the averaged angles of deflection of light $\langle \varepsilon_x \rangle$ in a turbulent flow behind a shock wave: a and c) dimension of the cell 12 × 12 mm and b and d) 3.5 × 3.5 mm; c) y = 124 and d) 160 mm. x, y, mm; $\langle \varepsilon_x \rangle$, seconds of arc.

discreteness of experimental data dependent on the period of the Talbot grid, we can write the absolute values of the refractive index in the submerged turbulent jet in recurrence form

$$\overline{n\,(x_i)} = n_0 - \sum_i \frac{n_0\,\langle \varepsilon_x \rangle_i}{\Delta z_i}\,\Delta x_i\,. \tag{1}$$

This distribution can be used for calculation of the averaged concentration of helium according to the procedure proposed in [12, 13]. Considering the helium-air mixture as a binary one and assuming that the values of the refractive index differ little from unity, we write Lorentz–Lorenz formulas in the form of the system of equations

$$\overline{n-1} = 2\pi\left(\overline{N_1}a_1 + \overline{N_2}a_2\right), \tag{2}$$

where $\overline{N}_1 + \overline{N}_2 = \overline{N}$. The results of calculations of the averaged concentration of helium in the flow field of the submerged jet from formulas (1) and (2) are presented in Fig. 5.

Since the average values of the density of air behind the shock wave are easily calculated from the shock adiabat, the absolute values for the average refractive index and the density of the flow behind the shock wave are found using expression (1). From the experimental measurements of the angles of refraction of light (see Fig. 4), Fig. 6 gives results of the calculation of the time-averaged density of the flow behind the shock wave after the traversal of turbulizing grids with cells of 12 × 12 mm (Fig. 6a and c) and 3.5 × 3.5 mm (Fig. 6b and d). It is seen that the bound-

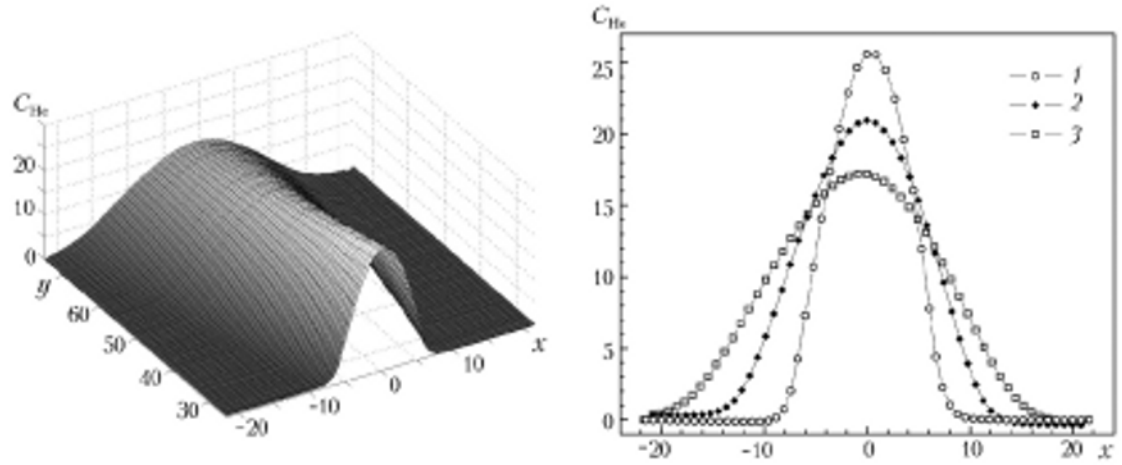

Fig. 5. Distribution of the averaged concentration of helium in the jet: 1) y = 30, 2) 50, and 3) 70 mm. x, y, mm; C_{He}, %.

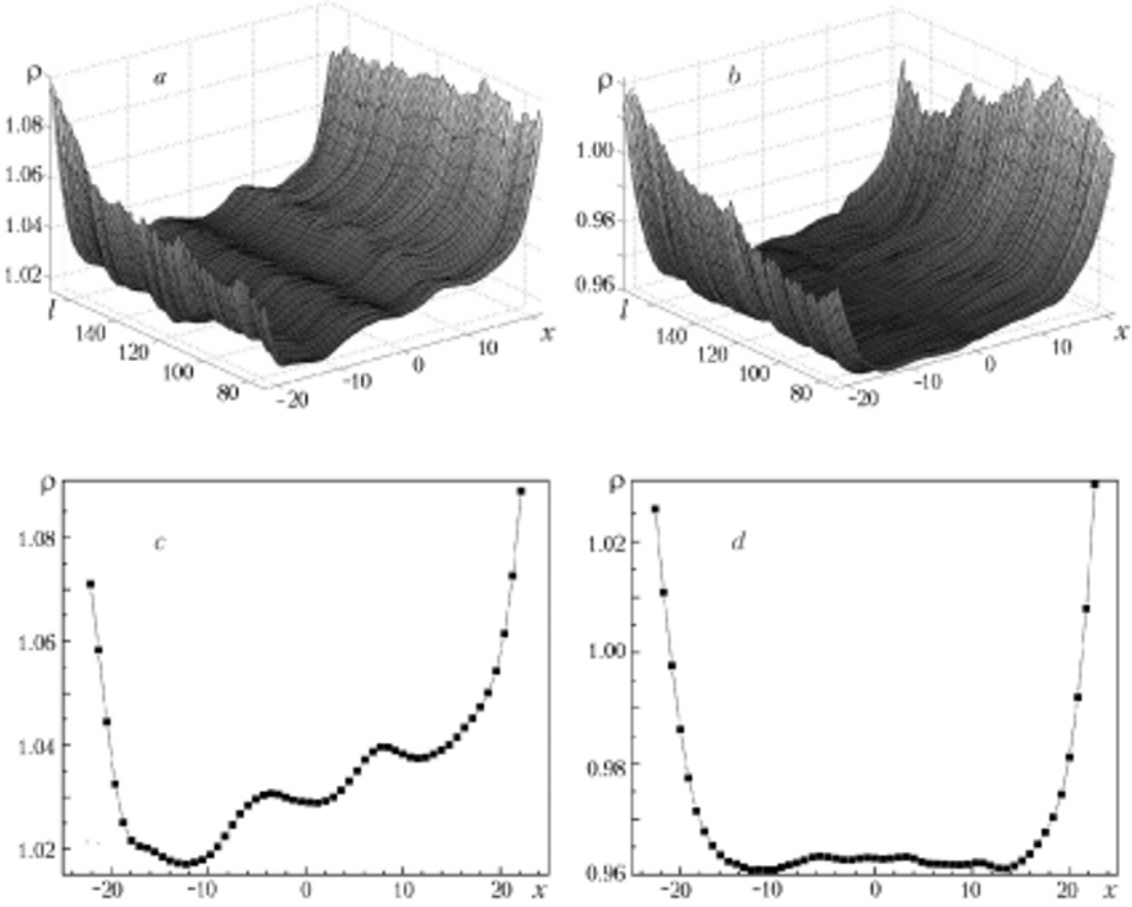

Fig. 6. Distributions of the averaged air density in the flow behind the incident shock wave: a and c) dimension of the cell 12 × 12 mm and b and d) 3.5 × 3.5 mm; c) y = 124, and d) 160 mm. x, y, mm; ρ, kg/m^3.

ary-layer thickness in the zone of observation is about 7–9 mm, whereas the gas density in the boundary layer grows compared to its average value in the flow core. This leads to an increase of 6–7% in the average flow density at a distance of ≈3 mm for the walls of the shock tube.

For the grid with a 3.5 × 3.5 mm cell (Figs. 4b and d and 6b and d), the dependence of the average angles of refraction on the coordinate across the tube channel is smoother. Unlike the grid with a large cell, we note the absence of appreciable density fluctuations in the core of the flow behind the shock wave (Fig. 6b and d). The reason can be either the specific character of turbulence or the insufficient sensitivity of the measuring circuit.

Conclusions. By the method of two-exposure Talbot photography, we have established the two-dimensional array of the angles of refraction of light in transmission by a two-dimensional turbulent submerged helium jet flowing out into an air space and a gas flow behind the front of the incident shock wave transmitted by turbulizing barriers.

The process of numerical processing of the structural distortions of Talbot images in the cases investigated enabled us to restore the averaged values of the concentration of helium over the flow field and the density of air over the cross section of the shock tube. It has been shown that the interaction in the wall boundary layer produces an increase of 6–7% in the average density of the flow at a distance of 3 mm from the tube walls.

This work was carried out with the financial support of the State Complex Scientific-Research Programs "Nanomaterials and nanotechnologies" and "Thermal processes."

NOTATION

a_1 and a_2, coefficients of polarizability of helium and air, m^3; C_{He}, relative concentration of helium, %; L, distance from the Talbot grid to the object under study, m; l, distance from the turbulizing grid to the measurement cross section, mm; M, Mach number; N_1 and N_2 concentrations of helium and air, m^{-3}; N, concentration of gas particles, m^{-3}; n_0, refractive index of admixture-free air; Re_l, Reynolds number; V, flow velocity, m/sec; x and y, running Cartesian coordinates, m; Δx_i, distance between the centers of neighboring unit Talbot elements, m; Δz_i, beam path length through the object under study, m; ρ, gas density, kg/m^3; ε_x and ε_y, local angles of deflection of light, seconds of arc.

REFERENCES

1. F. Talbot, Facts relating to optical science. IV, *Philos. Mag.*, **9**, 401–407 (1836).
2. J. Ebbeni, Nouveaux aspects du phenomene de moiré, *Nouv. Rev. Opt.*, **1**, No. 5, 333–342 (1970).
3. A. W. Lohmann and D. E. Silva, An interferometer based on the Talbot effect, *Opt. Commun.*, **2**, No. 9, 413–415 (1971).
4. Y. Nakano and K. Murata, Measurements of phase objects using Talbot effect and moire techniques, *Appl. Opt.*, **23**, No. 14, 2296–2299 (1984).
5. A. S. Koryakovskii and V. M. Marchenko, *On the Influence of Optical Inhomogeneities on the Reproduction of Periodic Distributions of the Coherent Field and of the ODGF Mode*, Preprint No. 89 of the Institute of Physics of the Academy of Sciences, Moscow (1979).
6. A. S. Koryakovskii and V. M. Marchenko, Interferometry of the optical inhomogeneities of the active media of lasers based on the Talbot effect, *Kvantovaya Élektron.*, **7**, No. 5, 1048–1057 (1980).
7. Yu. P. Voinov, G. M. Zuev, and A. S. Koryakovskii, On the possibility of investigating the optical quality of gas flows by the Talbot-interferometry method, *Kratk. Sobshch. Fiz.*, No. 1, 13–17 (1984).
8. A. S. Boreisho, A. S. Koryakovskii, and V. M. Marchenko, Investigation of the optical quality of the gas flows formed by nozzle blocks of honeycomb structure, *Zh. Tekh. Fiz.*, **55**, No. 10, 1943–1949 (1985).
9. C. Shakher, A. Daniel, and A. Nirala, Temperature profile measurement of axisymmetric gaseous flames using speckle photography, speckle shearing interferometry, and Talbot interferometry, *Opt. Eng.*, **33**, 1983–1988 (1994).
10. J. Stricker and B. Zakharin, 3-D turbulent density field diagnostics by tomographic moiré technique, *Exp. Fluids*, **23**, No. 1, 76–85 (1997).
11. C. Shakher and A. K. Nirala, A review on refractive index and temperature profile measurements using laser-based interferometric techniques, *Optics Lasers Eng.*, **31**, 455–491 (1999).

12. M. V. Doroshko, O. G. Penyaz'kov, G. Rénkin, P. P. Khramtsov, and I. A. Shikh, Investigation of a two-dimensional turbulent jet flow past a horizontal cylinder by the Talbot-interferometry method, *Heat and Mass Transfer–2005*, Minsk (2005), pp. 210–214.
13. M. V. Doroshko, O. G. Penyaz'kov, G. Rénkin, K. L. Sevruk, P. P. Khramtsov, and I. A. Shikh, Talbot-interferometry in measurements of the axisymmetric turbulent jet parameters, *Inzh.-Fiz. Zh.*, **79**, No. 5, 94–99 (2006).
14. M. V. Doroshko, P. P. Khramtsov, O. G. Penyazkov, and I. A. Shikh, Measurements of admixture concentration fluctuation in a turbulent shear flow using an averaged Talbot-image, *Exp. Fluids*, ISFV12 Special Issue (2006).